Demonstration of a concentrated solar power and biomass plant for combined heat and power

Jensen, Adam R.; Sifnaios, Ioannis; Perers, Bengt; Holst Rothmann, Jan; Mørch, Søren D.; Jensen, Poul V.; Dragsted, Janne; Furbo, Simon

Published in:
Energy Conversion and Management

Link to article, DOI:
10.1016/j.enconman.2022.116207

Publication date:
2022

Document Version
Publisher's PDF, also known as Version of record

Energy Conversion and Management 271 (2022) 116207

Contents lists available at ScienceDirect

Energy Conversion and Management

journal homepage: www.elsevier.com/locate/enconman

Demonstration of a concentrated solar power and biomass plant for combined heat and power

Adam R. Jensen [a,*], Ioannis Sifnaios [a], Bengt Perers [a], Jan Holst Rothmann [b], Søren D. Mørch [c], Poul V. Jensen [c], Janne Dragsted [a], Simon Furbo [a]

[a] Department of Civil and Mechanical Engineering, Technical University of Denmark, Koppels Allé, Building 404, 2800 Kgs Lyngby, Denmark
[b] Aalborg CSP A/S, Hjulmagervej 55, 9000 Aalborg, Denmark
[c] Brønderslev Forsyning A/S, Virksomhedsvej 20, 9700 Brønderslev, Denmark

ARTICLE INFO

Keywords:
Solar collector
Cogeneration
CHP
Bioenergy
Hybridization
Multi-generation

ABSTRACT

This study presents the design and performance of the Brønderslev hybrid plant – the world's first concentrated solar power (CSP)-biomass plant to utilize waste heat. The combined heat and power plant consist of a 16.6 MW parabolic trough collector field, two 10 MW biomass boilers, and an organic Rankine cycle (ORC) system with an electrical output of 4 MW. The solar collector field and biomass boilers are hydraulically connected and supply heat in parallel to the ORC system. A multi-stage heat recovery process ensures that the waste heat is supplied to the local district heating grid. The solar field can also be operated independently of the biomass plant, supplying heat directly to the district heating grid. The plant operation was investigated by analyzing measurements for 2020, and the monthly heat and electricity generation was calculated for each component. Additionally, the performance of the solar field and ORC was elucidated, and the ORC was found to have a maximum electrical efficiency of 20.6 %. Detailed results are shown for one day with joint heat supply to the ORC from the solar field and biomass boilers, and the corresponding energy flows are visualized using a Sankey diagram. The total efficiency of the biomass plant for the investigated year was 93.6 % based on the higher heating value of the fuel. Overall, it was found that the hybrid plant performed reliably and successfully demonstrated the potential of CSP-biomass hybridization.

1. Introduction

The world is currently undergoing a transition from reliance on fossil fuels to renewable energy sources. However, due to their intermittent generation profile, non-dispatchable renewables such as wind and solar cannot directly replace conventional baseload power [1]. The dispatchability of renewables can be increased by strategically combining two or more technologies, a concept known as hybridization. Hybridization also offers economic benefits due to joint infrastructure use and reduces the need for expensive energy storage [2].

According to a review by Pramanik and Ravikrishna [3], hybrid power plants have the potential to significantly reduce investment costs and increase efficiency compared to stand-alone systems. The study categorized hybridization schemes for concentrated solar power (CSP) according to renewable level (light, medium, and strong) and identified the possibility of coupling CSP with biomass, geothermal, wind, natural gas, and coal power plants.

Peterseim et al. [4] categorized CSP hybridizations according to three synergy levels: light hybrids (sharing of minimal infrastructure, e.g., transmission lines), medium hybrids (physically connected, but always requiring the operation of the host plant), and strong hybrids (sharing of major infrastructure/equipment with the option of independent CSP operation). The categorization of hybridization schemes is summarized in Fig. 1. Hybridization of CSP with coal and natural gas has a medium synergy level and a low to medium renewable level, whereas wind has a high renewable level but only a light synergy level. In contrast, hybridization of CSP and biomass has both a high renewable level and a strong synergy potential due to the sharing of Rankine cycle components.

Compared to stand-alone biomass plants, integration of CSP reduces biomass consumption while still being able to supply dispatchable power [5].

Economic investigations of CSP-biomass hybridization have shown that a cost reduction of more than 40 % is achievable when

* Corresponding author.
E-mail address: arajen@dtu.dk (A.R. Jensen).

https://doi.org/10.1016/j.enconman.2022.116207
Received 4 February 2022; Received in revised form 1 August 2022; Accepted 3 September 2022
Available online 10 October 2022

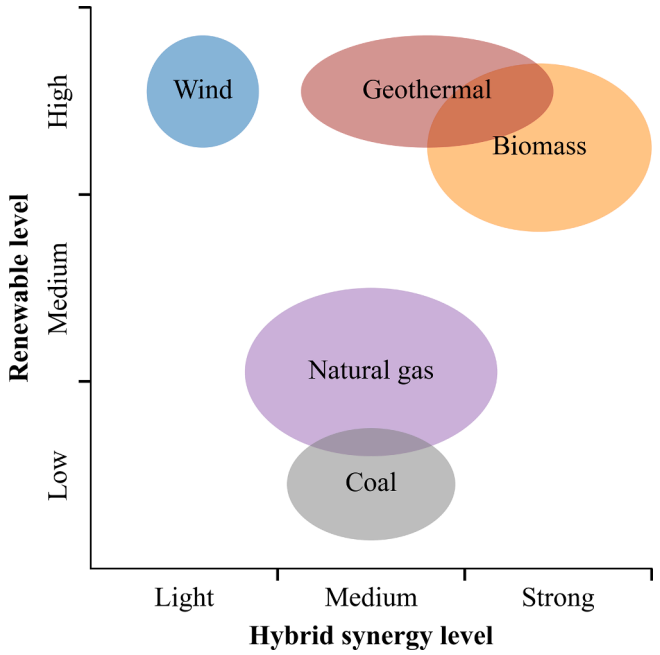

Fig. 1. Categorization of energy sources for CSP hybridization according to renewable level [3] and hybrid synergy level [4].

infrastructure is shared (e.g., turbine, generator, and grid connections) [6]. In addition to lower capital costs and being more profitable than conventional CSP systems, hybrid systems can have smaller footprints as the solar field can be made smaller [7]. Furthermore, Peterseim et al. [8] showed that the electricity efficiency of a conventional CSP system could be increased by 10 % by superheating with biomass, resulting in cost reductions up to 23 % for the investigated system configuration.

Apart from the economic benefit of CSP-biomass hybridization, the use of solar heat also has environmental benefits, as a carbon emission reduction ratio of 95.7 % can be achieved at design conditions [9]. An investigation of case studies of hybrid CSP-biomass plants indicated that such plants have economic and environmental benefits even in Nordic climatic conditions [10]. Nonetheless, for larger solar utilization and emission reduction, the use of long-term storage was suggested.

Hybrid systems can also be used for multi-generation, i.e., supplying multiple energy outputs. For example, Hashemian and Noorpoor [11] presented a CSP-biomass multi-generation system capable of generating electricity, heating, cooling, hydrogen, and potable water. Tsimpoukis et al. [12] investigated a trigeneration system supplying heating, cooling, and electricity utilizing CSP as the main energy source and biomass as a supplementary source. Similarly, Karellas and Braimakis [13] presented a model and economic analysis of a micro-scale hybrid plant able to operate as either a cogeneration or trigeneration plant.

Hussain et al. [14] investigated the suitability of different CSP technologies for hybridization with biomass, including solar tower, linear Fresnel reflector, Stirling dish, and parabolic trough collectors. While the expected economic performance was highest for solar tower and linear Fresnel reflector systems, parabolic trough collectors were generally favored in existing plants due to their high technological maturity level and modularity (suitable for small and large systems). Pantaleo et al. [15] also investigated CSP-biomass plants and identified the low economic profitability as the major drawback of the technology attributed to the high cost of CSP.

1.1. Hybrid CSP and biomass plants

The earliest proposal to combine CSP and biomass was made in the 1980s [16]. However, it was first decades later that the first CSP-biomass hybrid plant, the Termosolar Borges, was commissioned. The plant was completed in 2012 and, at the time, was the northernmost CSP plant in Spain [17].

The Thermosolar Borges consisted of 336 parabolic trough collectors (183 120 m^2) circulating thermal oil [18]. The thermal oil was heated to 400 °C and used to generate steam. Subsequently, the steam was superheated to 520 °C by the dual biomass boilers (2 × 22 MW_{heat}) to achieve a higher conversion efficiency [19]. The steam was used to power a 24.8 MW_{el} turbine, with an efficiency of 37 % at full load [20]. While the plant was completed, it was not connected to the electrical grid when the authors visited the plant in 2017, and the plant was subsequently destroyed in a fire in 2019.

In 2014, a second hybrid CSP-biomass plant was commissioned in Rende, southern Italy [18]. Specifically, an existing biomass plant was retrofitted with 9780 m^2 of linear Fresnel reflector collectors. The collectors were also used to heat a thermal oil, but only up to 280 °C. At this temperature level and plant size, steam turbines tend not to be an optimal choice; thus, the plant was connected to a 1 MW_{el} organic Rankine cycle (ORC) turbine.

Additionally, a prototype hybrid CSP-biomass plant was constructed in Tunis, Tunisia, as part of the REELCOOP project [21]. The plant consisted of 1000 m^2 parabolic trough collectors with an outlet temperature of 175 °C. Similar to the plant in Rende, the heat was used to power an ORC turbine (65 kW_{el}), which had a nominal electrical efficiency of 14 %.

To date, none of the CSP-biomass plants have utilized the waste heat of the power cycle but instead relied on a cooling infrastructure to dispose of the heat. For example, the Thermosolar Borges plant used wet cooling, in which heat is dissipated to the atmosphere using water evaporation.

Furthermore, the plants in Tunis and Rende utilize ORC turbines, as they are cheaper than steam turbines and tend to be economically favorable for small plants (<5 MW_{el}) [22]. While conceptually similar to the steam Rankine cycle, the organic Rankine cycle differs in that it uses a high-molecular organic fluid with a low boiling point instead of water/steam. One advantage is that it allows ORC turbines to generate electricity from lower-temperature heat sources. Also, due to the lower pressure and simpler design, ORC turbines do not require an on-site operator and consequently are attractive for decentralized power generation despite a lower efficiency than steam turbines [23].

For these reasons, ORC turbines have also been used with several stand-alone CSP plants, of which the first was the Saguaro Power Plant, commissioned in 2005 in Arizona, USA [24]. A comprehensive review of ORC systems worldwide has been presented in [25], an extensive review of ORC configurations, applications, and working fluids is presented in [26], and an overview of CSP-ORC plants is given in [27].

The most significant drawback to ORC turbines is their low electrical efficiency (typically between 15 and 23 %). However, this concern is alleviated when the waste heat is utilized, i.e., combined heat and power (CHP). By utilizing the waste heat, e.g., for district heating, the total plant efficiency can reach 88 % or even higher [23].

Nonetheless, as previously mentioned, all of the existing hybrid CSP-biomass plants do not utilize waste heat. The utilization of waste heat has so far only been theoretically studied. For example, Sterrer et al. [28] investigated retrofitting existing biomass CHP plants with a CSP field, with the main aim of displacing biomass consumption. While potentially economically attractive, the study concluded that numerous technical questions remain unanswered, and future research should focus on detailed planning of CSP fields and control strategies for optimum feed-in of solar thermal energy to the ORC.

1.2. Aim and novelty

In this study, we present the design and performance of a novel hybrid CSP-biomass plant integrated with an ORC turbine. The Brønderslev hybrid plant is the world's first CSP-biomass plant to provide combined heat and power, and its innovative design represents a

significant advancement in the field. The waste heat from the plant is utilized for district heating. The plant is also distinctive from other plants in that the CSP field and biomass boilers are hydraulically connected, meaning they use the same heat transfer fluid and, in parallel, supply heat to the ORC.

In this paper, results from one full year of operation are presented. Specifically, the heat and electricity production are analyzed on a monthly basis. The performance of the CSP field, biomass plant, and ORC are elucidated. Additionally, preliminary results from one day of joint heat supply from the CSP and biomass boilers are presented, including the operating conditions and illustration of energy flows.

2. Methods

The Brønderslev combined heat and power (CHP) plant is a hybrid district heating plant located in the town of Brønderslev in Northern Jutland, Denmark (latitude: 57.255 °N, longitude: 9.955 °E). The hybrid plant combines CSP and biomass combustion to produce heat and electricity. An aerial photo of the plant is shown in Fig. 2, with the CSP field, biomass plant, and outdoor biomass storage.

The district heating network is briefly described in Section 2.1, followed by an overview of the hybrid plant and the existing gas-powered plant in Section 2.2. Next, the major parts of the hybrid plant are introduced: the solar collector field in Section 2.3, the biomass units in Section 2.4, and the ORC in Section 2.5. Last, the monitoring setup is described in Section 2.6.

2.1. District heating network

The district heating network in Brønderslev consists of 160 km of piping and supplies heat to 4800 customers, of which the majority are residential houses. The average forward temperature is 74 °C, and the average return temperature is 35 °C.

Over the past five years, the annual heating production has been 122 GWh on average, with transmission losses accounting for 23 %. As an example, the daily average heat production and demand (including transmission losses) are shown in Fig. 3 for 2020. The production corresponds to the heat generated by the plant and solar field, some of which can be stored, whereas the demand is the actual heat supplied to the town. The figure illustrates a large variation in the heating demand caused by a strong seasonal trend in the ambient air temperature.

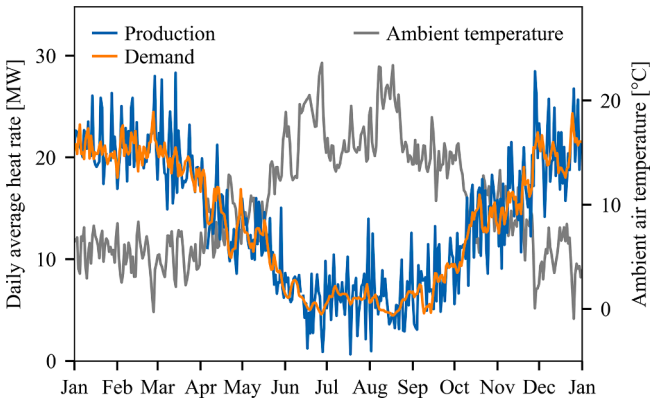

Fig. 3. Average daily heat production and demand for 2020.

2.2. System overview

The hybrid plant integrates a 16.6 MW_{heat} parabolic trough collector field and a 20 MW_{heat} biomass plant with a 3.9 MW_{el} organic Rankine cycle (ORC) system [29]. The solar field and biomass boilers heat up a thermal oil and, in parallel, supply heat to an ORC system, producing electricity and supplying district heating. The biomass plant features an advanced energy recovery system, which results in a very low flue gas exhaust temperature and high total plant efficiency.

The main reason for building the hybrid plant was to be able to deliver sustainable and affordable heat to the local community. Notably, switching to biomass and solar-based heat production helped avoid a planned price increase that was otherwise expected due to the discontinuation of the subsidy given to natural gas CHP plants in Denmark in 2019. The total price of the hybrid plant was 44 million EUR. The hybrid plant was designed with an aim to deliver 90 % of the town's district heating needs. The remaining heat is supplied by the existing natural gas-based CHP plant, henceforth referred to as the central plant. The central plant was kept primarily for producing heat during peak load hours and periods with favorable electricity prices. The interconnection of the hybrid and central plants is shown in Fig. 4.

Fig. 2. Aerial view of the solar collector field, biomass plant, and outdoor biomass storage area belonging to the Brønderslev hybrid plant. *Image source: the Danish Agency for Data Supply and Efficiency.*

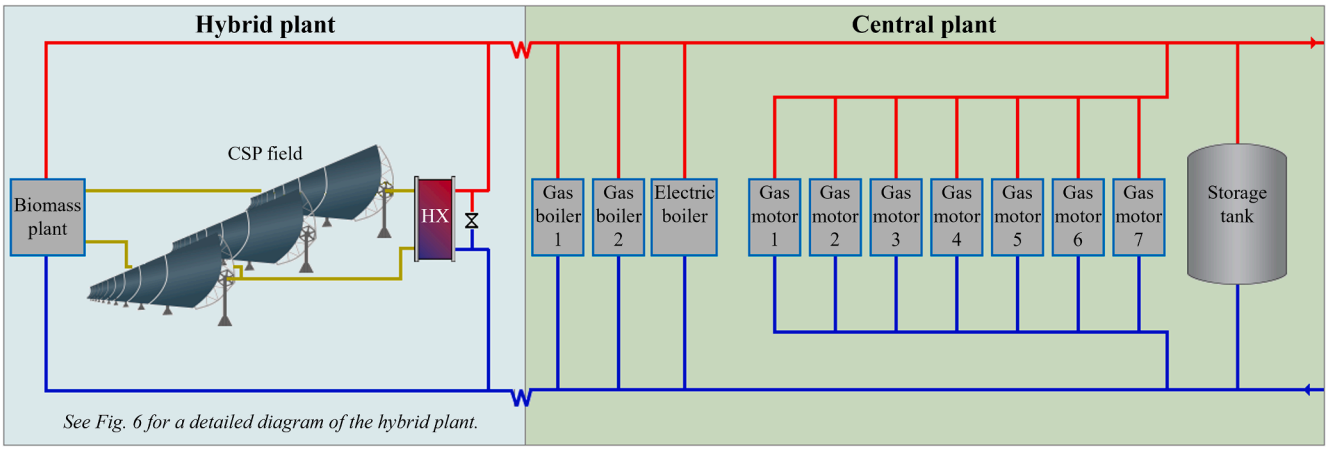

Fig. 4. Schematic of the interconnection of the biomass plant, solar field, and the existing central plant. The forward side (hot) of the district heating loop is shown in red, and the return side (cold) is shown in blue. The CSP thermal oil loop is shown in yellow. (For interpretation of the references to color in this figure legend, the reader is referred to the web version of this article.)

The central plant features seven gas motors with a combined effect of 22.8 MW_{el} / 30 MW_{heat} and two backup natural gas boilers with a combined effect of 30 MW_{heat}. The plant also includes a 20 MW_{heat} electric boiler, which is operated when the electricity price is low or negative, typically during periods with large amounts of wind power generation. To allow for flexible operation and supply of heat during maintenance periods, the central plant also has an 8 000 m^3 accumulation tank (corresponding to a heat capacity of 450 MWh_{heat}). As shown in Fig. 4, the gas motors, gas boilers, electric boiler, and storage tank are connected in parallel. The high technology diversity allows for dispatching the most cost-effective technology at any given time and safeguards against fuel price fluctuations and changes in taxation.

2.3. Solar collector field

The solar collector field is made up of 40 parabolic trough collectors (PTC) and has a peak thermal output of 16.6 MW_{heat}. On average, the solar field is expected to have an annual heat production of 16.0 GWh [30]. The collectors were installed during the fall of 2016 and were operational from January 2017. The solar field is located adjacent to the biomass power plant to reduce the length of piping (see Fig. 2) and covers an area of approx. 9 ha. In total, the investment cost of the CSP field was 11.6 million EUR.

The parabolic trough collectors are of the type AAL-Trough^{TM} 4.0 and manufactured by Aalborg CSP, who also delivered the control system for the solar field. The PTCs consist of large curved mirrors that focus the direct irradiance onto evacuated receiver pipes at the focus point. The receivers, manufactured by Huiyin, are 4 m long with a 70 mm diameter stainless steel absorber. Convection and conduction losses are minimized as the annulus between the absorber and glass envelope is evacuated. A close-up photo of the parabolic troughs is shown in Fig. 5, and the main parameters of the collectors and collector field are given in Table 1.

The 40 collectors are arranged in 10 parallel loops connected to a common forward and return pipe. Each loop consists of four collectors in series, resulting in a high flow rate through the receivers, which minimizes the possibility of overheating. Additionally, each loop features a separate temperature and flow controller, ensuring a stable temperature in the common return pipe from the CSP field.

The parabolic troughs are single-axis tracking, along an axis 29.9° east of north (see Fig. 2). While a north–south tracking axis gives the highest annual energy yield, this was not possible due to the shape of the available plot of land, hence the current orientation. The distance between the collector rows is 15 m, corresponding to a ground cover ratio of 0.36. The mirrors and receivers had not been cleaned since the installation of the collectors.

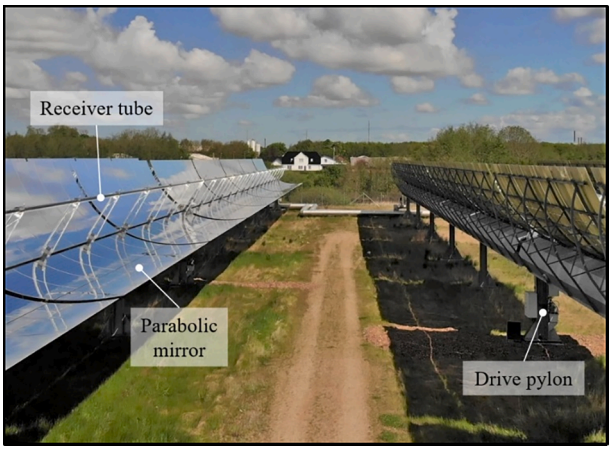

Fig. 5. Close-up photo of the parabolic trough collectors.

Table 1
CSP field and collector parameters.

Parameter	Value
Annual DNI	1 040 kWh/m^2
Total aperture area	26 930 m^2
Row spacing	15 m
Field orientation	29.9° east of north
Cost of CSP field	11.6 million EUR
Maximum collector temperature	340 °C
Mirror width	5.77 m
Collector length	125 m

2.3.1. Heat transfer fluid

Thermal oil is used as the heat transfer fluid, as this allows for high temperatures at low pressure. Specifically, Therminol 66 is used, which is a commercially available high-temperature synthetic oil -suitable for use in the range of -3 to 345 °C [31]. Being able to use the same heat transfer fluid in the CSP field and the biomass plant was a key reason for choosing Therminol 66, as this allowed the two systems to be directly coupled. The oil flow from the two systems is merged in a vertical header (illustrated in Fig. 6), which supplies heat to the ORC. This configuration allows for joint or separate supply of heat from the CSP field and biomass units to the ORC.

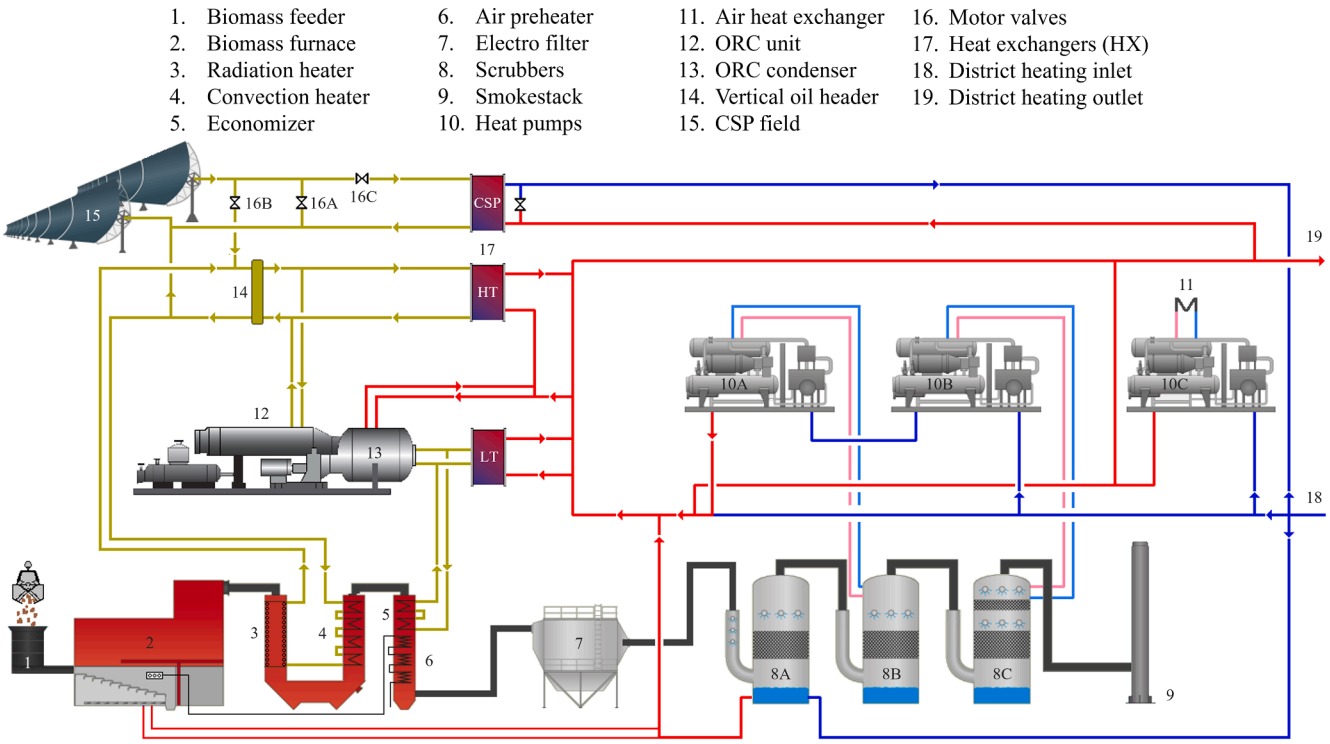

Fig. 6. Simplified schematic of the hybrid plant. The thermal oil loop is represented by the yellow lines, and the district heating loop is represented by the red (hot) and blue (cold) lines. Only one of the two identical biomass units is shown for simplicity. (For interpretation of the references to color in this figure legend, the reader is referred to the web version of this article.)

2.3.2. *Operating modes*

Depending on the irradiance level, the solar collector field can be operated in ORC or district heating mode. In the ORC mode, high-temperature heat is supplied to the ORC, and the solar field outlet temperature is set to match the heat supply from the biomass boilers (up to 312 °C). In the district heating mode, the outlet temperature setpoint is lower (typically around 190 °C) to reduce heat losses, and all of the produced heat is directly transferred to the district heating grid. As there is no storage for the thermal oil, the generated heat has to be discharged to either the district heating network or the ORC system. The heat supplied to the district heating network can be stored in the low-temperature DH storage tank.

2.3.3. *Control strategy*

In both modes, the flow rate in the solar collector field is controlled by a feed-forward controller. The flow rate resulting in the desired outlet temperature is determined based on the expected heat generation (derived from the measured irradiance and ambient temperature) and the temperature measured after each trough. The minimum flow rate in the CSP field is set to 40 % of the pump capacity to avoid overheating during rapidly changing weather. The maximum flow rate in the collector field is 495 m^3/hr.

The flow from the collector field can be either supplied to the district heating heat exchanger, the ORC, or recirculated. The diversion of the fluid is controlled using three motor valves (A-C), shown in Fig. 6. In the district heating mode, motor valves A (bypass loop) and B (ORC) are closed, and valve C (district heating) is fully open. By not recirculating any fluid, the lowest possible outlet temperature is achieved. In this mode, the flow rate and outlet temperature are controlled by adjusting the pump effect.

The control strategy is more complicated in the ORC mode as a high temperature to the ORC has to be maintained within a narrow band. First, it is necessary for the CSP field to heat up to the ORC setpoint temperature, which is done while in the district heating mode. As the field temperature approaches the setpoint, a small amount of fluid is circulated to the ORC to preheat the pipes. Then, gradually more flow is supplied to the ORC. At this time, only a small amount of fluid is supplied to district heating (motor valve C is set to 10 %). The outlet temperature is now controlled by adjusting the split between motor valves A and B, e.g., if the irradiance decreases, recirculation is increased (motor valve A), while the flow to the ORC is decreased (motor valve B).

Furthermore, the collectors are only set to track when there is sufficient irradiance, which is defined as when the pyrheliometer sensor has measured above 120 W/m^2 for at least five minutes.

2.4. *Biomass plant*

The biomass plant consists of two units with a nominal effect of 10 MW_{heat} each. Only one of the two units is shown in Fig. 6, as they are connected in parallel and are identical. Two smaller units were chosen instead of one large unit, as this setup offers greater flexibility and redundancy. Additionally, the biomass units are able to operate down to 30 % part-load. Each biomass unit consists of a furnace, fuel feeder, boiler (radiation and convection heater), electro filter, scrubbers, ash transport system, and a shared smokestack (see Fig. 6).

Wood chips - a waste product from local forestry logging - are used as fuel for the biomass plant. The wood chips come primarily from pine but also include several other tree varieties. The wood chips have an average water content of 42 % and a higher heating value of 11.83 GJ/tonne. Biomass delivery occurs daily for most of the year by truck and is either deposited in the outdoor biomass storage or unloaded directly into the indoor storage facility. Two fuel-feeding cranes transport the biomass from the indoor storage facility to the feeder. The biomass is then automatically fed into the moving-grate furnace by a hydraulic press and moved further along using the grates. The grates are cooled using district heating water to avoid slagging problems.

Flue gas from the biomass combustion exits the furnace at around 950 °C. The hot flue gas enters the first stage of the boiler, the radiation

heater, and subsequently the second stage, the convection heater. The boiler heats the high-temperature (HT) thermal oil loop, which is the primary heat supply to the ORC. The HT loop operates at a constant flow of 220 m^3/hr, except during startup and shutdown. The flue gas temperature is reduced to 300 °C in the boiler before entering the economizer. The economizer is connected to the low-temperature (LT) thermal oil loop, which also supplies heat to the ORC. After the economizer, the flue gas preheats the air being fed to the furnace.

Next, the flue gas enters the electro filter, which removes dust particles by inducing an electric field. At this stage, the flue gas has a temperature of around 146 °C, which is sufficient to heat the district heating water directly. Thus, the water from the first scrubber is coupled to a heat exchanger that preheats the district heating water (8A in Fig. 6).

While the flue gas exiting the first scrubber still contains a considerable amount of energy, it cannot be used to heat the district heating water due to its lower temperature (43 °C). Therefore, the thermal energy of the water from the two last scrubbers is instead used as the heat source for two heat pumps (combined capacity of 2 MW_{heat}). Additionally, the warm air in the plant is used as the heat source for a third smaller heat pump. The flue gas exiting the last scrubber has a temperature of around 16 °C and is ejected to the ambient through the smokestack. The multi-stage heat recovery process results in a very high heat recovery rate, low exhaust temperature, and consequently, a high efficiency.

2.5. Organic Rankine cycle (ORC) unit

The ORC unit is a Turboden 40 CHPRS Split with an electrical output of 3.9 MW_{el}. The ORC has an electrical efficiency of 19.3 % under nominal conditions (see Table 2).

The power cycle is a regenerative Rankine cycle using an organic fluid (hexamethyldisiloxane). First, the organic fluid in liquid form is pumped to the pressure level of the hot side of the cycle by the feed pump. After the feed pump, the fluid stream is split in two, where one part is heated in the regenerator, and the other is heated by the low-temperature (LT) thermal oil loop. The split-cycle configuration represents state-of-the-art and allows for more energy to be extracted from the flue gas, thereby increasing the plant's total efficiency.

Next, the fluid is vaporized in the evaporator using heat from the high-temperature (HT) loop. The generated vapor then expands into the turbine, which is directly connected to the generator, generating electricity. The fluid exiting the turbine still has a high energy content, which is partially recovered in the regenerator. Last, the fluid is condensed in the water-cooled condenser (using district heating water) and enters the feed-in pump, closing the loop.

As district heating water is used as the cooling fluid in the condenser, the outlet temperature of the organic fluid is limited by the district heating temperature. Therefore, the condenser temperature is significantly higher for ORC units with CHP, which results in reduced electrical output and lower electrical efficiency.

In contrast to stand-alone CSP-ORC operation, hybridization with biomass allows the plant to run 24/7, avoiding daily startup and shutdown of the ORC. However, when it is required for the ORC to start up or shut down, two heat exchangers, which connect the LT and HT loops to the district heating loop (Fig. 6), are employed. These heat exchangers are also utilized to supply heat directly from the biomass boilers to the district heating loop when the ORC is not in operation. As the ORC generally operates for months at a time, the energy transferred in these two heat exchangers is very low.

Originally, a subsidy scheme for renewable energy technologies granted the hybrid plant a fixed electricity price above the varying market price. However, prior to the plant's inauguration, the subsidy scheme was found to not be in compliance with EU regulations and was thus declared invalid. Instead, the plant now receives a feed-in tariff of 139 EUR/MWh under a different scheme.

Table 2
Nominal operating conditions and performance of the ORC unit.

Parameter	Value
HT thermal power ($Q_{oil,ht}$)	18.55 MW_{heat}
HT inlet/outlet temperature	238/312 °C
LT thermal power ($Q_{oil,lt}$)	1.85 MW_{heat}
LT inlet/outlet temperature	135/238 °C
ORC condenser inlet/outlet temperature	40/69 °C
ORC condenser thermal power ($Q_{dh,orc}$)	16.06 MW_{heat}
Nominal electric power output ($E_{orc,net}$)	3.93 MW_{el}
Nominal electrical efficiency ($\eta_{orc,el}$)	19.3 %
Total ORC efficiency ($\eta_{orc,total}$)	98 %

2.6. Monitoring setup

The performance of the biomass plant and CSP field has been analyzed based on monitoring data from 2020. For most of the year, the CSP field operated in district heating mode due to the change in the subsidy scheme, which meant that the supply of heat to the ORC from the CSP field was prohibited. Nevertheless, joint heat supply from the CSP field and biomass boilers to the ORC was demonstrated during four days in 2020. Therefore, only preliminary results of joint CSP-biomass operation are presented.

The heat supply on the primary side (thermal oil) was measured for the CSP field, from the CSP field to the header, and for the HT and LT loops. The thermal power was derived from the measured flow rate and the forward and return temperatures. Specifically, the temperatures were measured with immersed PT100 Class A sensors with an uncertainty of ± 0.7 K. The flow rates were measured with Siemens Sitrans FUS SONO / FUS060 flowmeters with a stated accuracy of ± 0.5 %. However, due to the use of constant thermal properties in the energy meters, there is a negative bias in the thermal power of around 5 %.

On the secondary side (district heating loop), the thermal power was measured individually for all components, i.e., grate cooling, the first scrubber, all three heat pumps, and the heat exchangers shown in Fig. 6. The heat generation of all the units at the central plant was also measured. Each energy flow was derived from two immersed PT100 temperature sensors with an uncertainty of ± 0.7 K and an electromagnetic flowmeter (Siemens SITRANS FM MAG 5000 / MAG 3100). The flow meters on the district heating side were rated Class 3 according to the European Standard EN1434, though the uncertainty of the flow meters was verified once a year and found to be below 1.5 %.

Furthermore, the fuel-feeding cranes were outfitted with a built-in scale that measured the weight of each load of biomass deposited into the fuel feeder. The direct normal irradiance (DNI) was measured with a Class A pyrheliometer (EKO MS-56) in the CSP field. The pyrheliometer was mounted on a solar tracker (EKO STR-21G) at the top of a 10-m weather tower shown in Fig. 2. Due to infrequent cleaning, the pyrheliometer experienced soiling of more than 30 % throughout parts of the measurement period. Therefore, only irradiance measurements from the following ten days after the cleaning of the pyrheliometer were considered. The measurements of the hybrid plant were made with a frequency of 1 s and stored as 2-minute average values. The measurements from the CSP field and the central plant were stored as 1-minute and 10-minute average values, respectively.

Based on the measurements, the electrical efficiency of the ORC was calculated on an hourly basis:

$$\eta_{orc,el} = \frac{E_{orc,net}}{Q_{in,orc}} \quad (1)$$

The electrical efficiency is the ratio of the net electricity generation relative to the thermal input power to the ORC.

$E_{orc,net}$ is the net electrical power output of the ORC and was defined as:

$$E_{orc,net} = E_{orc,gross} - E_{orc,aux} \quad (2)$$

where $E_{orc,gross}$ is the electrical power measured at the generator terminals, and $E_{orc,aux}$ is the auxiliary power consumption of the ORC. $Q_{in,orc}$ is the total thermal power input to the ORC and can be calculated as the sum of the thermal power transferred from the HT and LT boilers to the ORC and the heat from the CSP field to the ORC ($Q_{oil,csp}$). The heat from the HT boiler to the ORC is equal to the total heat generation of the HT boiler ($Q_{oil,ht}$) minus the heat supplied from the HT loop directly to the DH loop ($Q_{dh,ht}$). Similarly, the heat from the LT boiler to the ORC is equal to the total heat generation from the LT boiler ($Q_{oil,lt}$) minus the heat directly transferred to the DH loop ($Q_{dh,lt}$).

$$Q_{in,orc} = (Q_{oil,ht} - Q_{dh,ht}) + (Q_{oil,lt} - Q_{dh,lt}) + Q_{oil,csp} \quad (3)$$

Due to the high uncertainty of the thermal power supplied from the HT and LT oil loops, the ORC input power was instead estimated from the outputs of the ORC – district heating ($Q_{dh,orc}$) and electricity ($E_{orc,net}$) – and the total ORC efficiency ($\eta_{orc,total}$). The total ORC efficiency quantifies the heat losses from the ORC components and is assumed independent of the operating conditions since lower electricity production results in higher heat recovery and vice versa.

$$Q_{in,orc} \approx \frac{Q_{dh,orc} + E_{orc,net}}{\eta_{orc,total}} \quad (4)$$

where $Q_{dh,orc}$ is the thermal power transferred to the district heating loop from the ORC condenser and $\eta_{orc,total}$ is the nominal total efficiency of the ORC (98 %).

Furthermore, the total efficiency of the biomass plant was calculated as:

$$\eta_{total} = \frac{Q_{dh} + E_{orc,net}}{m_b \cdot HHV_b} \quad (5)$$

where Q_{dh} is the combined district heating thermal power from the biomass plant (includes the district heating generation of the ORC, heat pumps, scrubbers, and DH heat exchangers). m_b is the mass of the consumed biomass, and HHV_b is the higher heating value of the biomass. The total efficiency represents the ratio of the total energy outputs (sum of electricity and district heating generation) relative to the energy inputs. Note that the total efficiency was calculated for the biomass in stand-alone operation due to the limited joint CSP-biomass operation. The electricity consumption of secondary components (e.g., pumps, heat pumps, and motor valves) was not considered.

3. Results and discussion

Results are presented for the overall system, i.e., the hybrid and central plant, in Section 3.1. This is followed by a detailed investigation of the performance of the biomass plant in Section 3.2, the CSP field in Section 3.3, and the ORC in Section 3.4. Next, preliminary results of joint ORC-biomass operation are presented in Section 3.5, followed by an analysis of the electricity production and consumption in Section 3.6.

3.1. System performance

At any given time, the district heating demand needs to be met. However, since the storage tank provides short-term decoupling of heat consumption and production, the production does not always need to directly match the demand in the short term (demonstrated in Fig. 3 and Fig. 7). This flexibility allows for heat production to be optimized by dispatching units when the electricity price is favorable and maximizing the use of solar thermal heat.

An example of the heat production profile during five days is illustrated in Fig. 7. The generation mix varies considerably during this period, with the majority of the heat being supplied by the biomass plant on the first day, by the gas and electric boilers on the second and third day, and by a mix of solar heat, gas boiler, and gas motor operation over the last two days.

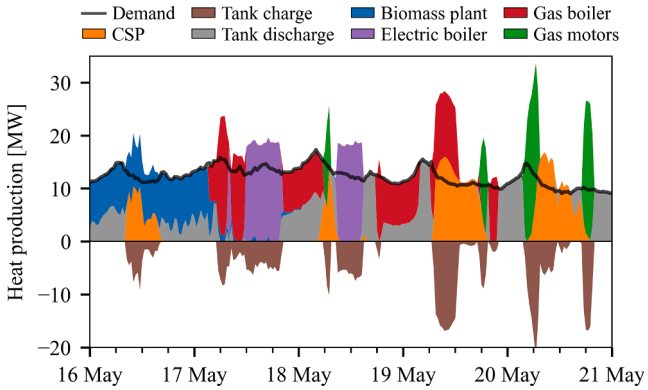

Fig. 7. Heat production by source during five days in May 2020.

The tank operation is also demonstrated in Fig. 7, with discharging of the tank occurring when the production is lower than the demand and charging when the production exceeds the demand. In addition to providing backup and a stable heat supply, the tank allows for storing surplus heat during the day that can be discharged during the night. For example, on May 19th, the solar and gas boiler heat generation exceeded the demand for several hours, during which the storage was charged. Later during the evening and night, the tank discharge supplied the entire demand for several hours. The storage also provides economic value during periods of high electricity prices where it is favorable to operate the gas motors. For example, the electricity price was very high during the morning of May 20th; hence, the gas motors were operated at high capacity resulting in increased revenue.

Furthermore, each source's monthly district heat production is shown in Fig. 8 for 2020. From this figure, it is evident that the biomass plant provided baseload during most of the year and thus produced the largest share of heating. However, the biomass units are shut down during the summer months, as the heat demand is low and the solar heat generation is high.

3.2. Energy production from the biomass plant

The monthly district heating contributions from the biomass plant are shown in Fig. 9 for 2020 (the components are illustrated in Fig. 6). The figure shows that both biomass units operated until the beginning of May, whereas only Biomass Unit 1 operated during the second half of the year. The reason for this was that Biomass Unit 2 was taken out of

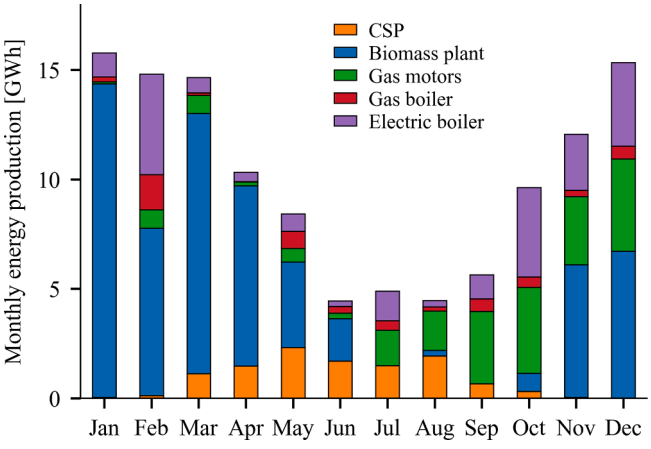

Fig. 8. Monthly heat production by source for 2020.

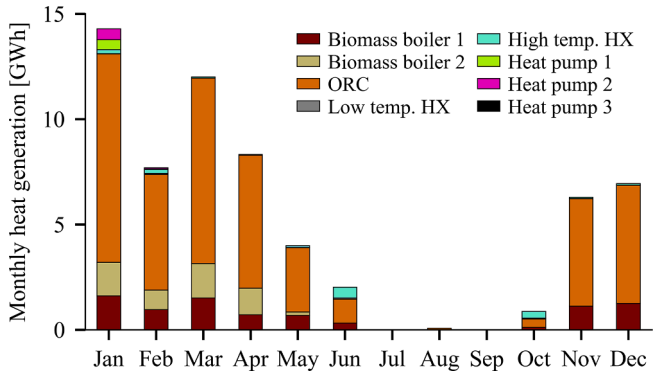

Fig. 9. Monthly heat generation of the biomass plant by component for 2020.

operation in order to rebuild the biomass feeder and combustion control system. To make up for the lower heat production from the biomass plant, the gas motors and electric boiler were used extensively from September to December (see Fig. 8).

When looking at the individual heat contributions from the biomass plant, the ORC was by far the largest contributor of heat to the district heating loop. The second largest contribution was from the biomass units, which refers to the direct heat supplied from the grate cooling and the first scrubber. The high-temperature (HT) and low-temperature (LT) heat exchangers (HX) only contributed a small amount of heat, as they are primarily used during the startup and shutdown of the ORC.

Additionally, during January and the beginning of February, the heat pumps supplied heat; however, after mid-February, all three heat pumps were out of service due to damage from fluid entering the compressor. When the heat pumps were not in operation, a significant amount of energy was lost, as the flue gas exiting the chimney was around 42 °C. In comparison, when the heat pumps were in operation, the average exhaust flue gas temperature was reduced to 20 °C. Thus, the plant's total efficiency for 2020 is not expected to reach the design values.

Nevertheless, the heat production from the hybrid plant accounted for approximately half of the heat production in 2020. In fact, the annual gas consumption was reduced to 4.1 million Nm^3 (normal gas cubic meter) in 2020 from an annual average consumption of 14.3 million Nm^3 during 2011–2017. This corresponds to an annual reduction of 31440 tonnes CO_2 (under the assumption that biomass is CO_2 neutral).

The biomass consumption was 23430 tonnes during 2020, and the combined heat and electricity production from the biomass plant was 72033 MWh. Consequently, the total efficiency of the biomass plant, η_{total}, was 93.6 % with respect to the higher heating value.

3.3. Solar collector field performance

The heat production from the solar collector field was 11.3 GWh for 2020. This corresponds to 420 kWh/m^2 or 9.5 % of the annual heat demand. Fig. 8 shows that the solar heat production was highly seasonally dependent, e.g., during the summer, the monthly solar thermal fraction reached up to 43 %. Overall, the solar field has operated reliably during the four years since its installation, with only minimum maintenance.

A comparison of the daily solar heat generation and the in-plane direct irradiation is shown in Fig. 10. During the investigated period, the maximum daily heat production was 6.4 kWh/m^2, which is 172 MWh in absolute units. For the days shown in Fig. 10, the overall conversion ratio was 57.7 %, i.e., the fraction of incident irradiation converted to useful heat. It should be noted that the conversion ratio is higher on days with high irradiation; thus, the annual conversion ratio is expected to be lower than that of the investigated period.

Furthermore, as shown in Fig. 7, the heat produced by the solar field sometimes exceeds the demand. By comparing Fig. 10 and Fig. 3, it can

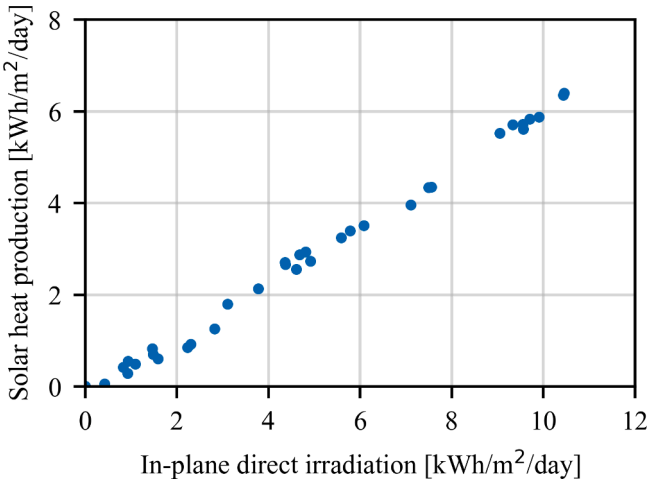

Fig. 10. Comparison of daily solar heat production and in-plane direct irradiation. Only days for which the pyrheliometer was cleaned within the last ten days are shown.

also be seen that the solar heat production can exceed the demand even on a daily basis. However, such high solar heat production is rare, as completely cloudless days are infrequent in Denmark. Even with a 30 % expansion of the solar collector field, curtailment is unlikely to be significant, as the large storage tank acts as a buffer between days of high and low irradiation.

Despite the reliable performance, the realized heat production from the CSP field (11.3 GWh) was substantially lower than predicted (16.0 GWh). The main reason for this is believed to be a large bias in the time series of direct normal irradiance used in the pre-construction prediction model (i.e., NASA's SSE irradiance dataset overestimated the available direct irradiance). This should serve as a reminder of the importance of using high-quality irradiance data.

In comparison, flat-plate solar collector fields in the same region generated on average 450 kWh/m^2 in the period 2012 to 2016 [32]. The output for 2020 is expected to be even higher due to the higher-than-average irradiation for the year. Regarding price, it can be noted that the nearby flat-plate collector field in Dronninglund required an investment cost of approximately 200 EUR/m^2 (about half the cost of the CSP field in Brønderslev) [33]. However, the heat generated by flat-plate collector fields is at a much lower temperature (typically with a mean temperature in the range of 60–70 °C). Nevertheless, the results indicate that parabolic trough collectors are not economically viable for direct district heating applications.

3.4. ORC operation

The electrical efficiency of the ORC, $\eta_{orc,el}$, is shown in Fig. 11 as a function of load fraction. The load fraction is defined as the heat supplied to the ORC relative to the nominal input (20.4 MW_{heat}). The maximum hourly electrical efficiency of the ORC was 20.6 %.

Fig. 11 shows a clear trend of increasing electrical efficiency with increasing load fraction. The degradation in the ORC performance from nominal load to 50 % load corresponds to a reduction of only 2.8 percentage points. However, at part-load below 30 %, the efficiency drops substantially. Similar findings were presented for a stand-alone biomass-ORC plant in [27].

The dispersion of the measurement points in Fig. 11 is due to different operating conditions, e.g., variation in temperature and flow rate in the thermal oil and district heating loop. The most influential parameter affecting the ORC electrical efficiency is the condenser temperature, illustrated by the color of the points in Fig. 11. Specifically, an increase in condenser temperature leads to an increase in the minimum pressure of the thermodynamic cycle and, consequently, a lower cycle

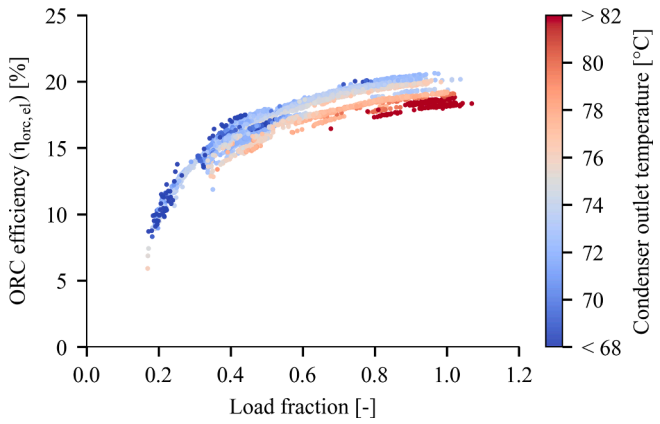

Fig. 11. ORC electrical efficiency as a function of the load fraction. Each point represents an hourly average and is colored according to the average condenser outlet temperature.

efficiency.

Prando et al. [34] found that the electrical efficiency of a biomass-ORC plant could be increased by one percentage point if the district heating forward temperature was decreased by 10 °C. Similarly, Fig. 11 shows an increase in efficiency of 1.5 percentage points when changing the condenser outlet temperature from 80 °C to 70 °C.

3.5. Joint CSP and ORC operation

Joint heat supply from the CSP field and biomass boilers to the ORC was demonstrated during four days in 2020. This section presents detailed results of the operation and performance of the hybrid plant for one of these days, namely May 5th, 2020.

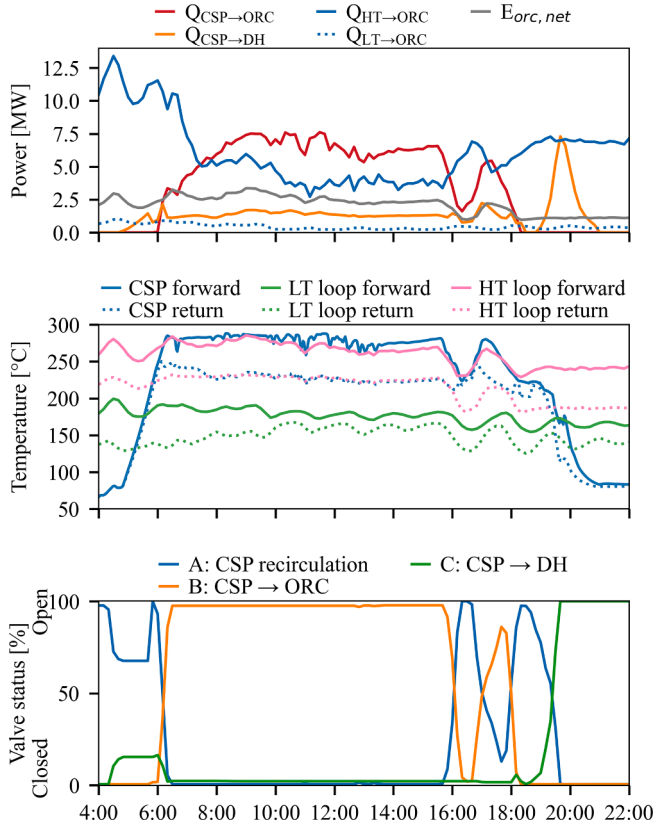

Fig. 12. Demonstration of joint supply of heat from the CSP field and biomass boilers to the ORC during May 5th, 2020. Time is in UTC.

The main system measurements of the hybrid plant are shown in Fig. 12, with the top subplot showing the thermal and electrical power. From the thermal power, it can be seen that the biomass units supplied heat during the entire day, though the heat output was significantly reduced around 7 am. Nevertheless, the electrical output from the ORC remained about the same until 3:30 pm due to heat supply from the CSP field.

The CSP field started operating in district heating (DH) mode around 5 am (see the middle and bottom subplot of Fig. 12). As the solar heat generation increased, the outlet temperature was gradually increased to the same temperature as the biomass boiler HT loop (285 °C). The high outlet temperature from the solar field was achieved by partly recirculating the heat transfer fluid in the CSP field, indicated by the relatively open motor valve A in the bottom subplot of Fig. 12. Once a sufficiently high outlet temperature was reached, the recirculation was gradually reduced, while the heat supply to the header was increased (motor valve B). The header is where the thermal oil from the CSP field and the oil from the two biomass HT loops merge, and from there, a single pipe supplies the ORC (see Fig. 6). Similarly, in the afternoon, the motor valves were used to control the outlet temperature of the solar field (though a decrease in temperature can be noticed shortly after 4 pm, which was caused by drifting clouds blocking the sun).

The energy flows during the entire day have been summarized in a Sankey diagram in Fig. 14. The figure illustrates how the two energy inputs (biomass and solar irradiation) are utilized. Approximately 61 % of the in-plane direct irradiation is converted to heat. The remaining energy is lost due to shading of the collectors (7 %) and optical and heat losses (32 %). Part of the heat from the CSP field was supplied to the ORC/header and some directly to the district heating grid.

Biomass, i.e., wood chips, is used as the fuel source for the biomass furnaces. As described in Section 2.4, the flue gas from the furnaces first enters the radiation heater and then the convection heater, heating the HT loop. The flue gas subsequently passes through the economizer, exchanging heat with the LT loop. The energy amounts exchanged in each step are shown in Fig. 14. The ORC is supplied by the HT and LT loops and generates electricity and district heating. During this particular day, the ORC operated with an average electrical efficiency of 18.4 % and a mean condenser outlet temperature of 75 °C. Heat losses from the ORC are assumed to be 2 % based on the ORC datasheet.

3.6. Electricity production and consumption

The monthly electricity production and consumption for the hybrid and central plants for 2020 are shown in Fig. 13. The electricity production from the ORC was significantly higher in the spring than in the fall, which was due to the second biomass unit being offline in the fall.

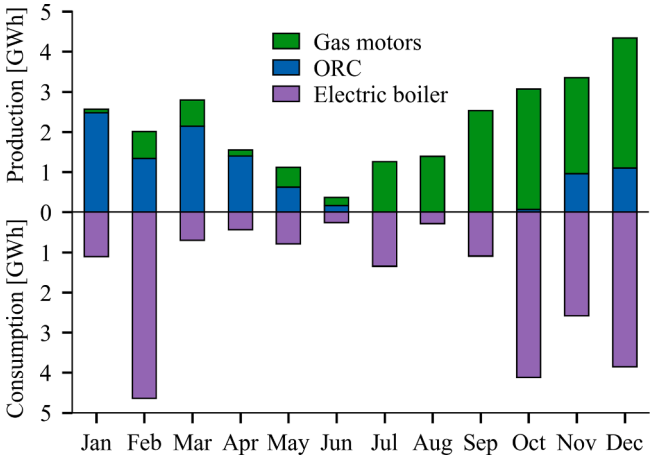

Fig. 13. Monthly electricity production and consumption for 2020.

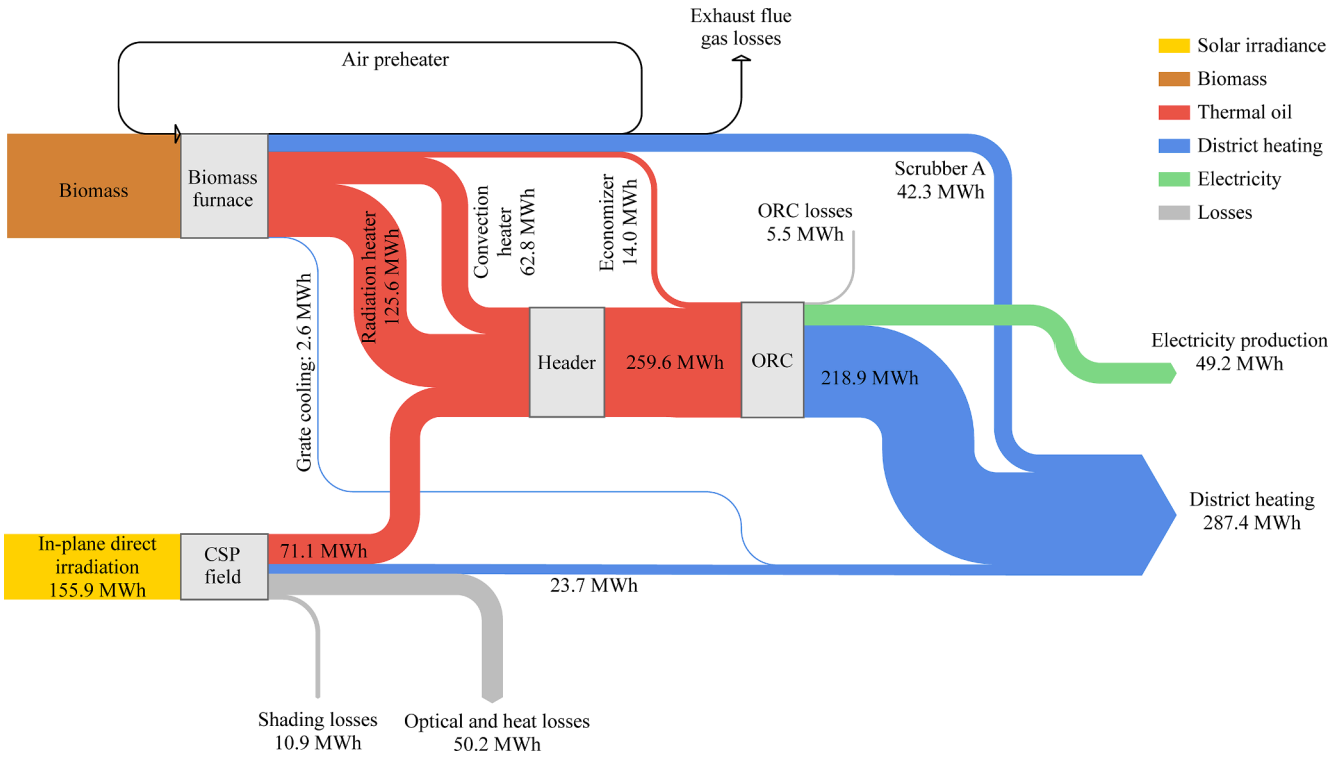

Fig. 14. Sankey diagram of the major energy flows in the hybrid plant during May 5th, 2020. Minor energy flows and various losses are not shown due to considerations of measurement uncertainty, e.g., HT and LT heat exchangers are not shown. Air preheating and flue gas losses (thin black lines) could not be calculated due to a lack of measurements. The heat pumps are not shown as they were not in operation.

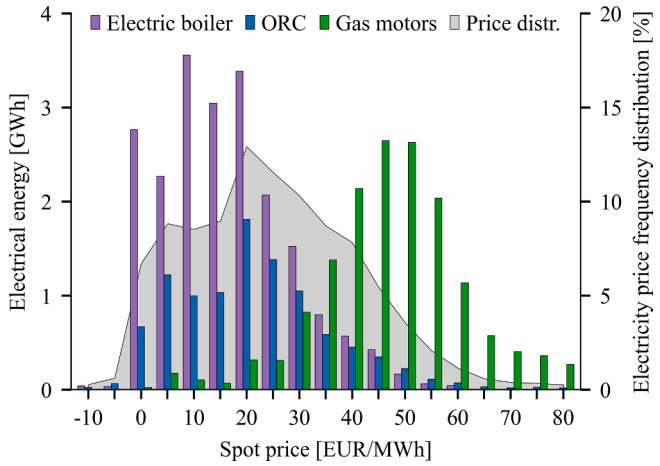

Fig. 15. Histogram of the electricity generation as a function of the hourly electricity spot price. The frequency distribution of the electricity price is shown in gray.

To compensate for the reduced heat supply from the biomass plant, the gas motors and the electric boiler were operated extensively from September to December.

In total, the ORC and gas motors generated 26.4 GWh of electricity, whereas the electric boiler consumed 21.2 GWh of electricity. However, it is important to consider that the electricity consumption and production did not occur simultaneously, as the units were dispatched strategically according to the electricity price.

A histogram of the electricity generation from the electric boiler, ORC, and gas motors as a function of the spot price is shown in Fig. 15. The figure shows very different distributions for the three sources. For instance, the average purchase price for the electric boiler was 16.0 EUR/MWh, differing significantly from the average annual electricity price of 24.8 EUR/MWh. This demonstrates how the electric boiler was primarily operated when the electricity price was low.

In comparison, the average price at which electricity was sold was 21.4 and 45.9 EUR/MWh for the ORC and gas motors, respectively. Again, this large price difference illustrates how the various technologies were operated differently.

Dispatching the electric boiler and gas motors according to the electricity price is possible as they have high ramp rates and can utilize the increased flexibility afforded by the storage tank. However, the biomass plant delivers baseload and has a much slower ramp rate; hence, the production distribution of the ORC closely matches the price distribution in Fig. 15, signifying that it is not strategically dispatched but rather operates more or less constantly. Calculations of the electricity consumption by the electric boiler were based on the assumption that the electric boiler has an efficiency of 99 %.

4. Conclusion

This study presented the design and performance of the Brønderslev hybrid plant – the world's first CSP-biomass plant to utilize waste heat. The plant features a field of parabolic trough collectors hydraulically connected with two biomass units that jointly supply high-temperature heat to an organic Rankine cycle (ORC) system.

The monthly district heat production from the hybrid plant was presented and compared to that of the existing gas-powered plant. In 2020, the hybrid plant supplied 73.0 GWh of district heating, corresponding to 61 % of the heat demand of the local town. Notably, the heat supplied by the hybrid plant resulted in a reduction in natural gas consumption by 10.2 million m^3 compared to previous years. The total annual efficiency of the biomass plant was found to be greater than 93 %. This shortcoming was mainly due to the heat pumps, which recover heat from the flue gas, being out of operation for most of the year.

Additionally, detailed results were presented for the ORC and the

CSP field. The performance of the ORC was found to be very close to the manufacturer's stated nominal electrical efficiency (19.3 %), with a maximum efficiency of 20.6 %. Furthermore, the solar field operated reliably and with limited maintenance requirements during the investigated period. During 2020, the solar field generated 11.3 GWh corresponding to 420 kWh/m^2. As the maximum monthly solar thermal fraction was only 43 %, there is potential for increasing the size of the solar field considerably, further reducing biomass and gas consumption.

Unfortunately, due to a change in regulation, there were very few days of joint CSP and biomass operation. Instead, the CSP field supplied heat directly to the district heating grid most of the time. However, joint CSP-biomass operation was successfully demonstrated for four days, and preliminary results and an operation strategy were presented. Additionally, the energy flows in the hybrid plant were presented for one full day of joint operation in the form of a Sankey diagram.

As joint CSP and biomass operation was very limited, several unanswered questions remain, including how the system's dynamic behavior and variable supply of heat due to short-term fluctuations influence the operation of the ORC. While this full-scale system has successfully demonstrated the technology, such systems still require subsidies to be profitable. As many ORC biomass plants exist in Europe, the limiting factor in hybridization with CSP is the cost of the CSP system. Therefore, future research should focus on lowering the costs of concentrating collectors in order for hybrid plants to become economically viable.

CRediT authorship contribution statement

Adam R. Jensen: Conceptualization, Methodology, Visualization, Investigation, Writing – original draft. **Ioannis Sifnaios:** Methodology, Visualization, Investigation, Writing – review & editing. **Bengt Perers:** . **Jan Holst Rothmann:** Conceptualization, Investigation, Writing – review & editing. **Søren D. Mørch:** Investigation, Writing – review & editing. **Poul V. Jensen:** Conceptualization, Writing – review & editing. **Janne Dragsted:** Supervision, Writing – review & editing. **Simon Furbo:** Supervision, Writing – review & editing, Funding acquisition.

Declaration of Competing Interest

The authors declare that they have no known competing financial interests or personal relationships that could have appeared to influence the work reported in this paper.

Data availability

The authors do not have permission to share data.

Acknowledgments

This work was supported by the Danish Energy Agency's Energy Technology Development and Demonstration Program (EUDP), grant no. 64015-0626.

References

[1] Ravestein P, Van Der SG, Haarsma R, Scheele R, Van Den BM. Vulnerability of European intermittent renewable energy supply to climate change and climate variability. Renew Sustain Energy Rev 2018;97:497–508. https://doi.org/10.1016/j.rser.2018.08.057.
[2] Powell KM, Rashid K, Ellingwood K, Tuttle J, Iverson BD. Hybrid concentrated solar thermal power systems: a review. Renew Sustain Energy Rev 2017;80:215–37. https://doi.org/10.1016/j.rser.2017.05.067.
[3] Pramanik S, Ravikrishna RV. A review of concentrated solar power hybrid technologies. Appl Therm Eng 2017;127:602–37. https://doi.org/10.1016/j.applthermaleng.2017.08.038.
[4] Peterseim JH, White S, Tadros A, Hellwig U. Concentrating solar power hybrid plants - Enabling cost effective synergies. Renew Energy 2014;67:178–85. https://doi.org/10.1016/j.renene.2013.11.037.
[5] Bai Z, Liu Q, Lei J, Wang X, Sun J, Jin H. Thermodynamic evaluation of a novel solar-biomass hybrid power generation system. Energy Convers Manag 2017;142:296–306. https://doi.org/10.1016/j.enconman.2017.03.028.
[6] Peterseim JH, Tadros A, White S, Hellwig U, Landler J, Galang K. Solar tower-biomass hybrid plants - Maximizing plant performance. Energy Procedia 2014;49:1197–206. https://doi.org/10.1016/j.egypro.2014.03.129.
[7] Middelhoff E, Andrade Furtado L, Peterseim JH, Madden B, Ximenes F, Florin N. Hybrid concentrated solar biomass (HCSB) plant for electricity generation in Australia: Design and evaluation of techno-economic and environmental performance. Energy Convers Manag 2021;240:114244. https://doi.org/10.1016/j.enconman.2021.114244.
[8] Peterseim JH, Tadros A, Hellwig U, White S. Increasing the efficiency of parabolic trough plants using thermal oil through external superheating with biomass. Energy Convers Manag 2014;77:784–93. https://doi.org/10.1016/j.enconman.2013.10.022.
[9] Wang J, Chen Y, Lior N, Li W. Energy, exergy and environmental analysis of a hybrid combined cooling heating and power system integrated with compound parabolic concentrated-photovoltaic thermal solar collectors. Energy 2019;185:463–76. https://doi.org/10.1016/j.energy.2019.07.027.
[10] Modi A, Bühler F, Andreasen JG, Haglind F. A review of solar energy based heat and power generation systems. Renew Sustain Energy Rev 2017;67:1047–64. https://doi.org/10.1016/j.rser.2016.09.075.
[11] Hashemian N, Noorpoor A. Assessment and multi-criteria optimization of a solar and biomass-based multi-generation system: thermodynamic, exergoeconomic and exergoenvironmental aspects. Energy Convers Manag 2019;195:788–97. https://doi.org/10.1016/j.enconman.2019.05.039.
[12] Tsimpoukis D, Syngounas E, Bellos E, Koukou M, Tzivanidis C, Anagnostatos S, et al. Investigation of energy and financial performance of a novel CO_2 supercritical solar-biomass trigeneration system for operation in the climate of Athens. Energy Convers Manag 2021;245:114583. https://doi.org/10.1016/j.enconman.2021.114583.
[13] Karellas S, Braimakis K. Energy-exergy analysis and economic investigation of a cogeneration and trigeneration ORC-VCC hybrid system utilizing biomass fuel and solar power. Energy Convers Manag 2016;107:103–13. https://doi.org/10.1016/j.enconman.2015.06.080.
[14] Hussain CMI, Norton B, Duffy A. Technological assessment of different solar-biomass systems for hybrid power generation in Europe. Renew Sustain Energy Rev 2017;68:1115–29. https://doi.org/10.1016/j.rser.2016.08.016.
[15] Pantaleo AM, Camporeale SM, Miliozzi A, Russo V, Shah N, Markides CN. Novel hybrid CSP-biomass CHP for flexible generation: thermo-economic analysis and profitability assessment. Appl Energy 2017;204:994–1006. https://doi.org/10.1016/j.apenergy.2017.05.019.
[16] McDonald CF. A hybrid solar closed-cycle gas turbine combined heat and power plant concept to meet the continuous total energy needs of a small community. J Heat Recover Syst 1986;6:399–419. https://doi.org/10.1016/0198-7593(86)90227-4.
[17] Cot A, Amettler A, Vall-Llovera J, Aguilo J, Arque JM. Termosolar Borges: A Thermosolar Hybrid Plant with Biomass. In: Third Int Symp Energy from Biomass Waste 2010.
[18] NREL. Concentrating Solar Power Projects 2021. https://solarpaces.nrel.gov/projects (accessed December 13, 2021).
[19] Peterseim JH, Hellwig U, Tadros A, White S. Hybridisation optimization of concentrating solar thermal and biomass power generation facilities. Sol Energy 2014;99:203–14. https://doi.org/10.1016/j.solener.2013.10.041.
[20] Overton TW. Termosolar Borges, Les Borges Blanques, Spain 2015. https://www.powermag.com/termosolar-borges-les-borges-blanques-spain/ (accessed December 13, 2021).
[21] Ferchichi S, Kessentini H, Morales S, Willwerth L, Soares J, Castro J, et al. Testing and Modeling of Direct Steam Generating Parabolic Trough Collectors. Freiburg, Germany: International Solar Energy Society; 2018. p. 1–12. https://doi.org/10.18086/eurosun2018.10.02.
[22] Karsten L, Hoffmann J, Dinter F. An Organic Rankine Cycle as technology for smaller concentrated solar powered systems. In: ISES Sol World Congr 2017 - IEA SHC Int Conf Sol Heat Cool Build Ind 2017, Proc 2017:85–96. https://doi.org/10.18086/swc.2017.04.05.
[23] Quoilin S, Van Den BM, Declaye S, Dewallef P, Lemort V. Techno-economic survey of organic rankine cycle (ORC) systems. Renew Sustain Energy Rev 2013;22:168–86. https://doi.org/10.1016/j.rser.2013.01.028.
[24] Canada S, Cohen G, Cable R, Brosseau D, Price H. Parabolic trough organic rankine cycle solar power plant. 2004 DOE Sol Energy Technol 2005;1:1–2. https://doi.org/10.2172/881481.
[25] Tartière T, Astolfi M. A world overview of the organic rankine cycle market. Energy Procedia 2017;129:2–9. https://doi.org/10.1016/j.egypro.2017.09.159.
[26] Rahbar K, Mahmoud S, Al-Dadah RK, Moazami N, Mirhadizadeh SA. Review of organic Rankine cycle for small-scale applications. Energy Convers Manag 2017;134:135–55. https://doi.org/10.1016/j.enconman.2016.12.023.
[27] Petrollese M, Cau G, Cocco D. The Ottana solar facility: dispatchable power from small-scale CSP plants based on ORC systems. Renew Energy 2020;147:2932–43. https://doi.org/10.1016/j.renene.2018.07.013.
[28] Sterrer R, Schidler S, Schwandt O, Franz P, Hammerschmid A. Theoretical analysis of the combination of CSP with a biomass CHP-plant using ORC-technology in Central Europe. Energy Procedia 2014;49:1218–27. https://doi.org/10.1016/j.egypro.2014.03.131.
[29] Jensen AR, Sifnaios I. Modeling, Validation, and Analysis of a Concentrating Solar Collector Field Integrated with a District Heating Network. Solar 2022;2(2):234–50. https://doi.org/10.3390/solar2020013.

[30] Zourellis A, Perers B, Donneborg J, Matoricz J. Optimizing efficiency of biomass - fired organic rankine cycle with concentrated solar power in Denmark. Energy Procedia 2018;149:420–6. https://doi.org/10.1016/j.egypro.2018.08.206.
[31] Eastman. THERMINOL 66 - heat transfer fluid 2019:1–8. https://www.therminol.com/sites/therminol/files/documents/TF-8695_Therminol-66_Technical_Bulletin.pdf (accessed January 15, 2022).
[32] Furbo S, Dragsted J, Perers B, Andersen E, Bava F, Nielsen KP. Yearly thermal performances of solar heating plants in Denmark – Measured and calculated. Sol Energy 2018;159:186–96. https://doi.org/10.1016/j.solener.2017.10.067.
[33] PlanEnergi. Sunstore 3 - Phase 2: Implementation. 2015.
[34] Prando D, Renzi M, Gasparella A, Baratieri M. Monitoring of the energy performance of a district heating CHP plant based on biomass boiler and ORC generator. Appl Therm Eng 2015;79:98–107. https://doi.org/10.1016/j.applthermaleng.2014.12.063.